



Gesellschaft für Umweltmeteorologie mbH

Documentation about the anemos wind atlas for Europe 10 km

anemos
Gesellschaft für Umweltmeteorologie mbH
Böhmsholzer Weg 3, D-21391 Reppenstedt
Tel.: 04131-8308-100
www.anemos.de | kontakt@anemos.de



| Inhaltsverzeichnis | Seite |
|---|-------|
| 1. Introduction..... | 3 |
| 2. The WRF model..... | 4 |
| 3. Input data | 5 |
| 4. Optimization of the model settings..... | 5 |
| 5. Statistical verification with wind measurements..... | 5 |
| 6. Literatur | 8 |

1. Introduction

The **anemos Windatlas** for Europe 10 km (**EU-10km.E5**) represents a database containing long-term time series for the atmospheric parameters wind speed, wind direction, air temperature, air pressure, relative humidity, air density, precipitation, long- and shortwave radiation. The temporal resolution of the wind atlas is 10 minutes, the horizontal resolution is 10 x 10 km². It completely covers Central Europe, as well as large parts of the Mediterranean and North & Baltic Sea. Fig. 1 shows the process chain of the development of the anemos wind atlas. The two main points are:

- Optimization of the model settings with subsequent WRF main simulation (Downscaling)
- Verification of the WRF main simulation with wind measurements

More detailed explanations of these points can be found in the following chapters.

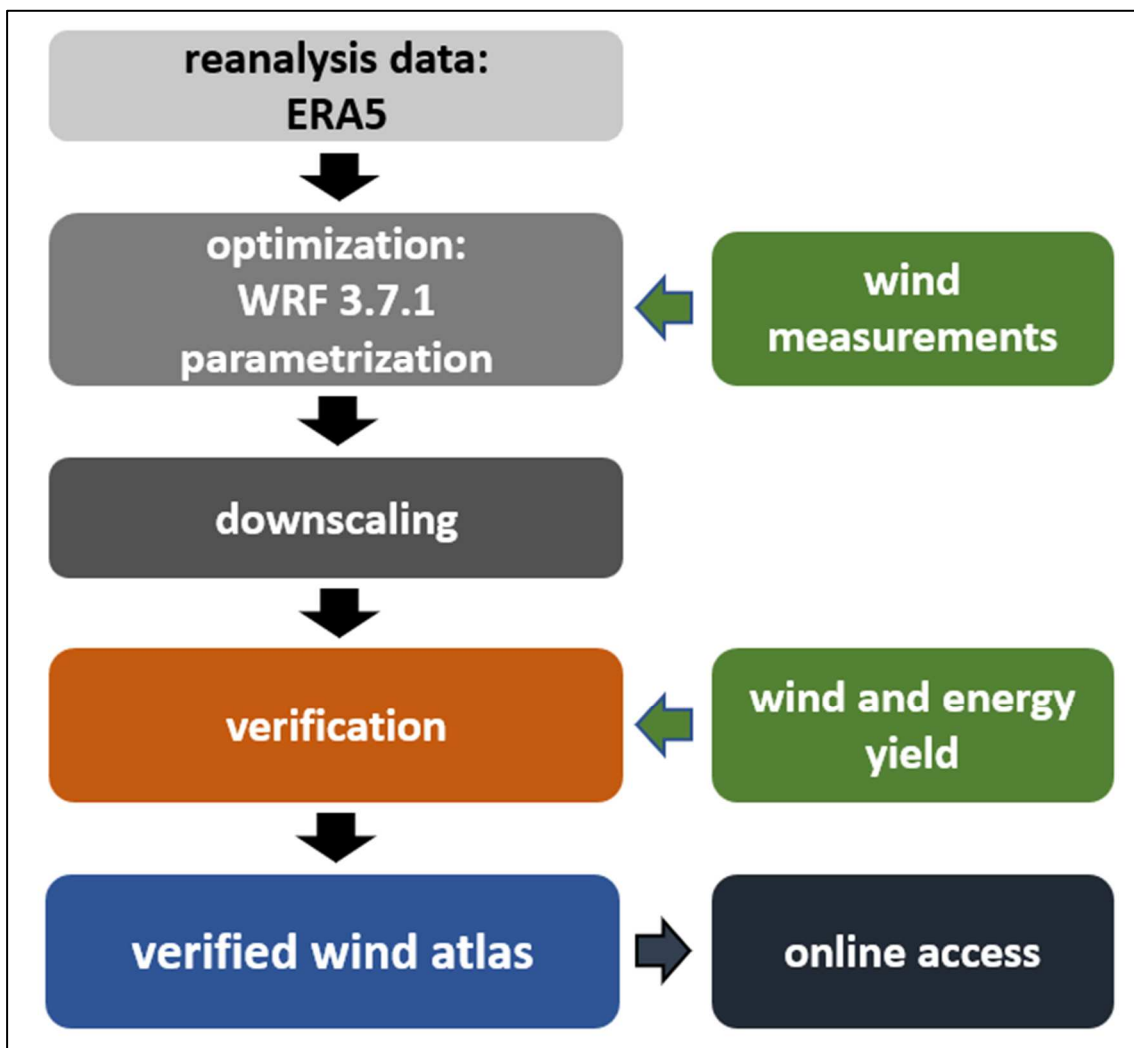


Fig. 1: Developmental steps of the anemos wind atlas for Europe 10 km.

2. The WRF model

The wind atlas **EU-10km.E5** is created by means of the meteorological mesoscale model **WRF** (**Weather Research & Forecasting Model with the Version 3.7.1**). The WRF model is a state-of-the-art weather forecast system (coupled atmospheric-land surface model) of the next generation which was developed in the 1990s at **NCAR** (**National Center for Atmospheric Research**).

WRF is a non-hydrostatic model (explicit calculation of the vertical velocity) and estimates for each time step the Navier-Stokes equations, which describe the atmospheric flow. Mesoscale processes such as the land-sea wind circulation can be sufficiently resolved by the model. However, microphysical processes as well as convection, radiation or planetary boundary processes have to be parameterized.



Fig. 2: Domain of the anemos wind atlas Europe 10 km. Domain with 10 x 10 km².

For the wind atlas **EU-10km.E5** one domain is applied (Fig. 2). The domain covers large parts of Europe and has a spatial resolution of 10 x 10 km².

During the simulation, new input data are assimilated into the WRF model every hour, which forces the model into the right direction (nudging process). The atmospheric state variables are stored every 10 minutes for each grid point on a grid. The simulation covers the period 1999 up to date and is continuously extended. The vertical model structure of the atmosphere has a high resolution with 50 vertical layers. The lower heights, which are relevant for wind turbines (up to 300 m) contain already 14 of the 50 vertical layers.

3. Input data

The WRF model requires surface data (soil temperature, soil moisture, snow, etc.) as well as all important atmospheric parameters (wind, temperature, pressure, relative humidity, etc.) as input data. For the wind atlas **EU-10km.E5** the worldwide available ERA5 reanalysis data are used as input and driving data. The ERA5 reanalysis data are of higher quality than the former ERA-Interim reanalysis data regarding consistency and correlation. Therefore, the advantages of the ERA5 reanalysis data such as consistency, homogeneity, length of time series, continuous updates, onshore as well as offshore availability can be preserved or even amplified by the WRF model. In addition, the disadvantages of relatively low spatial (approx. 30 x 30 km²) and temporal resolution (1 h) of ERA5 reanalysis data are surmounted by the anemos wind atlas **EU-10km.E5**.

The surface data are taken from the ERA5 data set as well. Thus, consistency of the radiation- and heat flow between surface and atmospheric is given. The surface data consists of four surface levels and contains i.a. soil moisture, soil temperature and snow.

The ground level elevations are taken from the **SRTM** data set (**S**huttle **R**adar **T**opography **M**ission, USGS EROS Data Center) and interpolated onto the model grid. These data were collected in the year 2000 and are available with a spatial resolution of about 90 m. The vertical resolution is 1 m. Any information about vegetation or roughness conditions within the boundaries of the simulation area are derived from the USGS data set (United States Geological Survey). The grid data are available in a spatial resolution of 1 km.

4. Optimization of the model settings

The model settings and parameterizations (e.g., planetary boundary scheme, surface scheme, radiation scheme) were tested prior to the main simulation and optimized for the relevant atmospheric parameters (wind speed and wind direction). The model settings were compared with the anemos wind atlas (D-3km.M2, D-3km.E5 etc.) and were verified with wind measurements (met masts and LiDAR, see Fig. 1). These tests show how the wind field near the ground reacts to different parameterizations and schemes (sensitivity tests). After that, the setting which yields the smallest deviations between model and observations was used for simulating the entire time period (> 20 years).

5. Statistical verification with wind measurements

The most important task after running the main simulation is its intensive verification with a variety of wind measurements. About 96 measurements were used for verifying the **EU-10km.E5**.

Through the verification the quality of the main simulation is determined. The verification includes statistical key parameters such as mean values, coefficient of determination (R^2) or correlation (R), bias, root mean squared error (RMSE) and extreme values (QQ-plot). Additionally, vertical profiles, diurnal cycles, wind roses, and frequency distributions with Weibull parameters are checked.

The rough distribution of the locations is shown by red circles in Fig. 3. Altogether 96 stations with measurements between 40 m and 140 m height are available. Additionally, the verification results of 75 measurements are shown in Fig. 4 for a measurement height of 100 m. For this purpose, the bias of the wind speed at four offshore and 71 onshore stations as well as the coefficient of determination (R^2 , hourly values) are calculated and graphically displayed. This allows a comparative evaluation between the measurements and the wind atlas. The boxes represent the 25 % - 75 % quartile, i.e. the middle 50 % of the data, and the whiskers (antennas) the minimum and maximum. The mean value (median) is marked by a cross (line in the box).

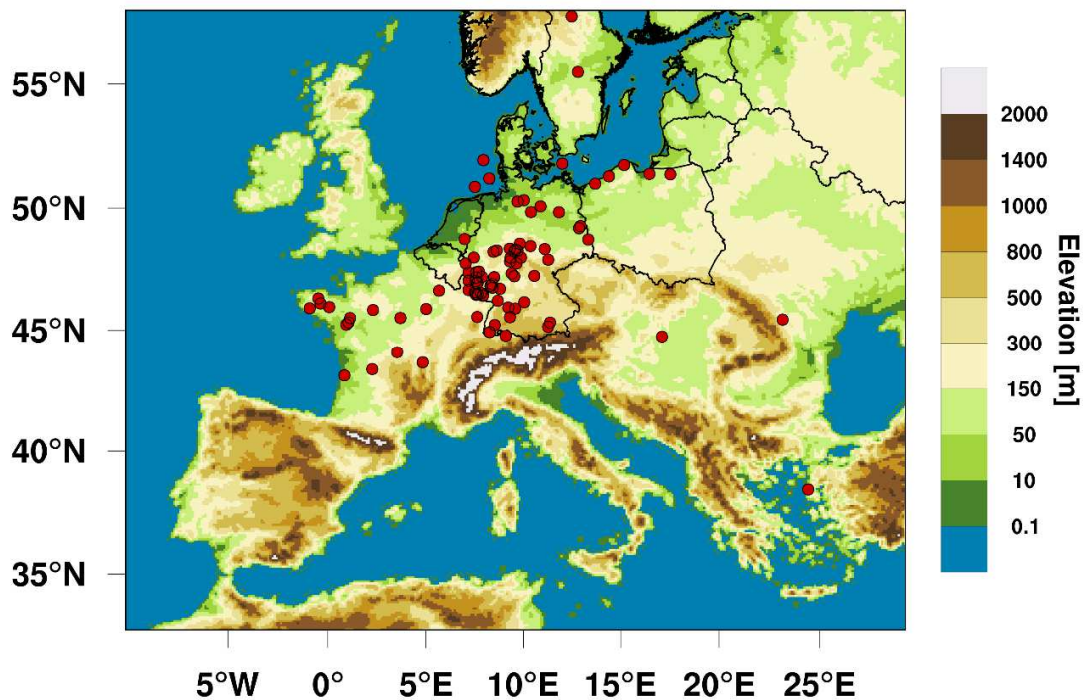


Fig. 3: Final model domain of anemos wind atlas Europe 10 km. The color bar shows the model elevation. Red circles mark roughly the 96 measurement sites.

First, the bias and the R^2 between measurements and simulation at the uppermost height (top anemometer) are considered. Fig. 4(a) shows that the mean bias is positive for the onshore measurements and negative for the offshore measurements. In addition, it can be seen that the R^2 is higher for the offshore sites than for the onshore sites (Fig. 4(b)). The bias is on average +10 % for the onshore stations. For the offshore measurements, the mean bias is -2.7 %. The standard deviation for all sites is 10.2 %. The R^2 for the offshore measurements is with 91.2 % significantly higher as the onshore measurements with 71.5 %.

Fig. 5(a) shows the deviation in percentage between the wind speed of each measurement and the 10 km wind atlas time series as well as the corresponding R^2 (Fig. 5(b)). The bias is on average 14 % for all stations. For the onshore measurements the mean bias is 15 % and for the offshore measurements -3 %. The standard deviation for all stations is 11.6 %. The R^2 of the offshore measurements with 91.2 % is significantly higher than the onshore measurements with 70.7 %.

Overall, the results show that the bias is lower when looking at the stations at 100 m than looking at the highest measurement height of a station. In addition, it is shown that R^2 is lower considering the 100 m height than the measurements at the highest measurement height. However, this can be explained by the fact that lower measurement heights have a higher error than upper measurement heights due to stronger soil influence. Therefore, the higher R^2 at the upper heights can be explained. Furthermore, it should be noted that the offshore locations improve the results with all measurements due to the lower bias and the higher R^2 .

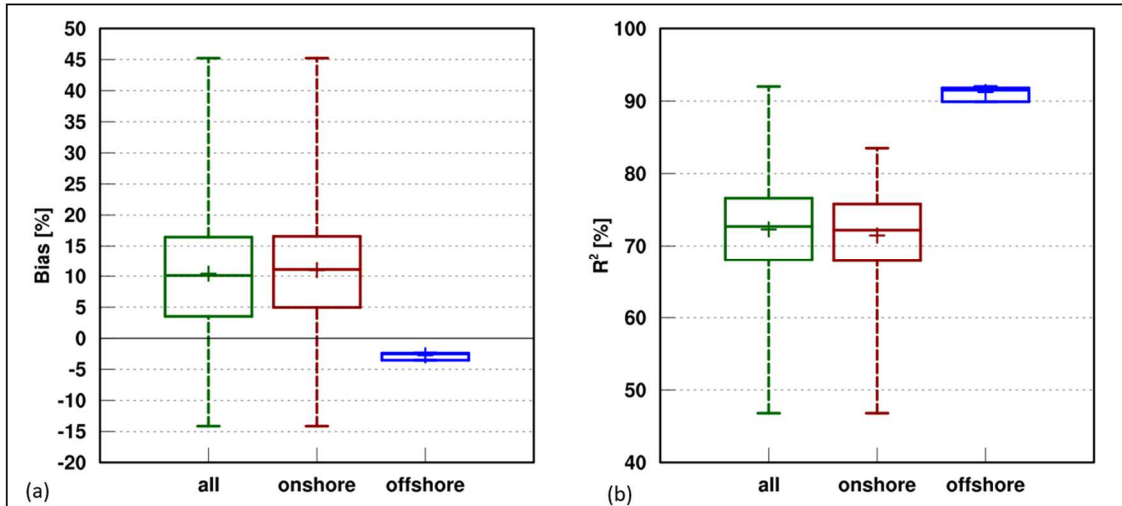


Fig. 4: Boxplot between 96 independent measurements and the anemos wind atlas at heights between 40 m and 140 m above ground. The bias (a) and the R^2 (b) are shown.

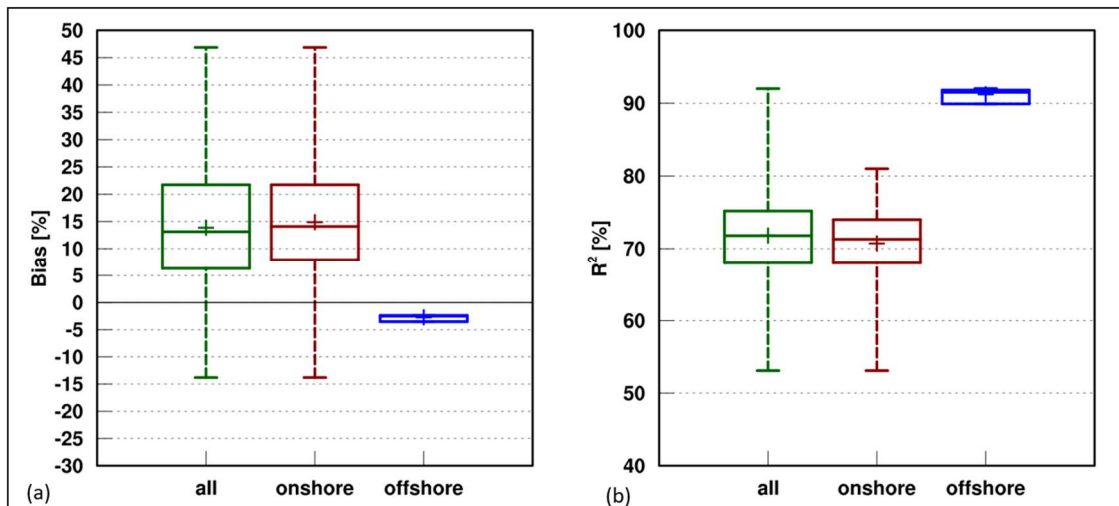


Fig. 5: Boxplot between 75 independent measurements and the anemos wind atlas at heights 100 m above ground. The bias (a) and the R^2 are shown.

6. Literatur

Christoffer, J. and M. Ulbricht-Eissing, 1989: Die bodennahen Windverhältnisse in der Bundesrepublik Deutschland, Bericht des DWD, Nr. 147

Copernicus Climate Change Service (C3S) (2017): ERA5: Fifth generation of ECMWF atmospheric reanalyses of the global climate . Copernicus Climate Change Service Climate Data Store (CDS), date of access. <https://cds.climate.copernicus.eu/cdsapp#!/home>

Farr, T. G., et al., 2007: The Shuttle Radar Topography Mission, Rev. Geophys., 45, RG2004, doi:10.1029/2005RG000183; <http://www2.jpl.nasa.gov/srtm/srtmBibliography.html>

Howard, Tom and Clark Peter, 2007: Correction and downscaling of NWP wind speed forecasts, Meteorol. Appl. 14: 105-116

Keil, M., M. Bock, T. Esch, A. Metz, S. Nieland, A. Pfitzner, 2010: CORINE Land Cover Aktualisierung 2006 für Deutschland. Abschlussbericht zu den F+E Vorhaben UBA FKZ 3707 12 200 und FKZ 3708 12 200, Deutsches Zentrum für Luft- und Raumfahrt e.V., Deutsches Fernerkundungsdatenzentrum Oberpfaffenhofen, Januar 2010

Mengelkamp, H.-T., 2015: Wind-, Ertrags- und Erlösgutachten für Windenergieanlagen, promet – meteorologische Fortbildung, Hrsg. Deutscher Wetterdienst, Jahrg. 39, Nr. 3/4, 193-202

Mengelkamp, H.-T., 1999: Wind Climate Simulation over Complex Terrain and Wind Turbine Energy Output Estimation, Theor. Appl. Climatol, 63, 129-139

Mengelkamp, H.-T., H. Kapitza and U. Pflüger, 1997: Statistical-dynamical downscaling of wind climatologies, Journal of Wind Engineering and Industrial Aerodynamics, 67&68, 449-457

Schneider, M., J. Bethke, A. Glücksmann, H.-T. Mengelkamp, 2016: Der neue anemos Windatlas für Deutschland – Korrektur und Verifikation mit Windmessungen und Ertragsdaten, 25. Spreewindtage, 09. November, Potsdam

Staffell, Iain and Pfenninger Stefan, 2016: Using bias-corrected reanalysis to simulate current and future wind power output, Energy 114, 1224-1239

Thogersen, M.L. et. al., Measure-Correlate-Predict Methods: Case Studies and Software Implementation, EMD International A/S

Traup, S. and B. Kruse, 1996: Winddaten für Windenergienutzer, Selbstverlag des Deutschen Wetterdienstes

Troen, I. and E.L. Petersen, 1989: European Wind Atlas. Risø National Laboratory, Roskilde. 656 pp. ISBN 87-550-1482-8

Weiter, A., M. Schneider, D. Peltret and H.-T. Mengelkamp: Electricity production by wind turbines as a means for the verification of wind simulations. Meteorol. Z. doi: 10.1127/metz/2019/0924

WRF, 2017, User's Guides for the Advanced Research WRF (ARW) Modeling System, Version 3, WRF users page, http://www2.mmm.ucar.edu/wrf/users/docs/user_guide_V3/contents.html